

Transepithelial Topography-Guided Ablation Assisted by Epithelial Thickness Mapping for Treatment of Regression After Myopic Refractive Surgery

Wen Zhou, MD, MSc; Dan Z. Reinstein, MD, MA(Cantab), FRCSC; Xiangjun Chen, MD, PhD; Shihao Chen, MD, OD; Yangyang Xu, MD, MSc; Tor Paaske Utheim, MD, PhD; Aleksandar Stojanovic, MD, PhD

ABSTRACT

PURPOSE: To evaluate the outcomes of transepithelial, topography-guided, epithelial mapping-assisted ablation in the treatment of regression after myopic refractive surgery.

METHODS: A retrospective consecutive case series of 70 eyes of 52 patients with regression after previous corneal refractive surgery for treatment of myopic and compound myopic astigmatism underwent re-treatment using transepithelial topography-guided and epithelial mapping-assisted custom ablation with a wide and smooth transition zone design. The ablation profile was based on data from corneal topography, whereas the epithelial ablation depth was decided by corneal epithelial mapping obtained by optical coherence tomography.

RESULTS: The mean follow-up time after re-treatment was 13.6 ± 9.4 months [range: 6 to 51 months]. At the patients' last

follow-up visit, 98.5% and 76.5% had uncorrected distance visual acuity of 20/40 and 20/20 or better. Safety and efficacy indexes were 1.05 and 0.92, respectively. The mean spherical equivalent was reduced from -1.10 ± 0.65 to -0.16 ± 0.34 diopters. Both total root mean square, odd-order, and even-order higher order aberrations improved significantly ($P = .021$, $.040$, and $.030$, respectively), whereas corneal asphericity remained unchanged ($P = .662$). Epithelial thickness profile showed significant smoothing between the central 2-mm and 2- to 5-mm paracentral areas.

CONCLUSIONS: Transepithelial topography-guided and epithelial mapping-assisted custom re-treatment with a wide and smooth transition zone design is safe and effective for addressing myopic regression in patients who have previously undergone myopic refractive surgery.

[J Refract Surg. 2019;35(8):525-533.]

The enhancement rate after primary laser refractive surgery varies widely in the literature. Rates ranging from 1.8% to 22%,¹⁻³ 2.3% to 5.2%,^{4,5} and 1.1% to 4.39%^{6,7} have been reported for laser in situ keratomileusis (LASIK), photorefractive keratec-

tomy (PRK), and small incision lenticule extraction (SMILE), respectively.

Residual refractive errors after laser refractive surgery remain the most common reason for patients' dissatisfaction and re-treatment. In addition, laser

From SynsLaser Kirurgi AS, Tromsø, Norway (WZ); London Vision Clinic, London, United Kingdom (DZR); the Department of Ophthalmology, Columbia University Medical Center, New York (DZR); Sorbonne Université, Paris, France (DZR); Biomedical Science Research Institute, University of Ulster, Coleraine, Northern Ireland (DZR); the Department of Ophthalmology, Arendal Hospital, Arendal, Norway (XC); Faculty of Health Sciences, National Centre for Optics, Vision and Eye Care, University College of Southeast Norway, Kongsberg, Norway (XC); Wenzhou Medical University, Wenzhou, China (SC, YX); the Departments of Medical Biochemistry Ophthalmology and Ophthalmology, Oslo University Hospital, Oslo, Norway (TPU); Department of Ophthalmology, Sørlandet Hospital, Arendal, Norway (TPU); the Department of Ophthalmology, Stavanger University Hospital, Stavanger, Norway (TPU); the Department of Clinical Medicine, Faculty of Medicine, University of Bergen, Norway (TPU); and Eye Department, University Hospital North Norway; Faculty of Clinical Medicine, University of Tromsø, Tromsø, Norway (AS).

Submitted: November 22, 2018; Accepted: July 30, 2019

Dr. Reinstein is a consultant for Carl Zeiss Meditec (Carl Zeiss Meditec, Jena, Germany) and has a proprietary interest in the Artemis technology (ArcScan Inc., Golden, Colorado) through patents administered by the Center for Technology Licensing at Cornell University (CTL), Ithaca, New York. The remaining authors have no financial or proprietary interest in the materials presented herein.

Correspondence: Aleksandar Stojanovic, MD, PhD, Eye Department, University Hospital North Norway, Sykehusveien 38, 9019 Tromsø, Norway. E-mail: aleks@online.no

doi:10.3928/1081597X-20190730-01

refractive surgery can also induce stromal irregularities, resulting in higher order aberrations (HOAs)^{8,9} and nonconformity between corneal and stromal surface due to epithelial remodeling.¹⁰⁻¹³ A custom procedure such as topography-guided treatment seems to be proper for the treatment of residual refractive errors and HOAs, and transepithelial phototherapeutic keratectomy (PTK) combined with topography- or wavefront-guided custom ablation has been reported to be effective in repairing irregular corneas.¹⁴⁻¹⁶ To specifically address the effect of HOAs and the epithelial remodeling induced by the primary treatment, data derived from corneal topography/tomography and corneal epithelial mapping were used as the basis for planning of the custom transepithelial surface ablation and evaluated in the current study.

PATIENTS AND METHODS

PATIENTS

Seventy eyes of 52 patients with residual myopia after laser refractive surgery for myopia or compound myopic astigmatism who underwent re-treatment by transepithelial topography-guided and epithelial mapping-assisted surface ablation were evaluated retrospectively. The re-treatments were performed between April 2010 and October 2017 at SynsLaser Clinic, Tromsø, Norway. The patients provided informed consent, and approval for anonymous use of the data was obtained from the Norwegian data authority. The need for ethics committee approval was waived due to the retrospective nature of the study.

The inclusion criterion for the re-treatment was patient dissatisfaction with uncorrected distance visual acuity (UDVA) due to residual myopia or myopic compound astigmatism. The exclusion criteria were: residual hyperopia with or without astigmatism; complications after the primary surgery; reported significant subjective visual disturbances such as halos and double vision that cannot be improved by spectacles or contact lenses; corrected distance visual acuity (CDVA) worse than 20/20; estimated stromal pachymetry after re-treatment of 300 μ m or less; and other eye pathology.

Patients underwent preoperative and postoperative ophthalmic examinations, which consisted of slit-lamp biomicroscopy, visual acuity/subjective manifest refraction (Nidek RT-2100 system; Nidek Co. Ltd., Aichi, Japan), Placido-based corneal topography and wavefront aberrometry (Nidek OPD Scan II; Nidek Co. Ltd.), dynamic pupillometry (pMetrics; iVIS Technologies, Taranto, Italy), and Goldmann applanation tonometry. Scheimpflug-based corneal topography/tomography by Precisio (iVIS Technologies) was performed under

“Refractive surgery” mode to ensure ± 3 μ m repeatability within the central 6 mm of the anterior corneal elevation. Corneal epithelial thickness mapping was obtained using the RTVue-100 26000-Hz optical coherence tomographer (OCT) (Optovue Inc., Fremont, CA).

SURGICAL PLAN

The transepithelial custom ablation was performed using iVIS Suite (iVIS Technologies), an integrated system consisting of the Precisio tomographer, pMetrics pupillometer, Corneal Interactive Programmed Topographic Ablation (CIPTA) planning software, and iRES excimer laser (iVIS Technologies).

The refractive ablation profile was compiled using subjective refraction and corneal topography data, aiming at achieving postoperative emmetropia and regularization of the anterior corneal optics. Subjective or total (ray-traced) corneal astigmatism was used in programming of astigmatism correction, depending on the amount and orientation of the lenticular astigmatism, which was estimated as a vectorial difference between intraocular astigmatism, measured by the OPD Scan II, and the posterior corneal astigmatism, measured by the Precisio. In cases where the estimated lenticular astigmatism corresponded to the difference between the subjective and total corneal astigmatism, the subjective astigmatism was used as the end point for the astigmatic correction; otherwise total cornea astigmatism was used. The size of the optical zone of the refractive ablation was based on the size of the entrance pupil measured by dynamic pupillometry. A custom transition with gradually decreasing refractive effect, connecting the optical zone and the peripheral cornea outside the treatment area, was designed by the CIPTA for each hemimeridian. This topography-guided, homogeneous transition along all hemimeridians yielded a larger total treatment zone of customized size and shape. Detailed principles of the concept are described elsewhere.^{16,17}

Epithelial thickness map obtained by the RTVue-100 was used to assist in the determination of the lamellar ablation depth, whereas the diameter and shape of the lamellar ablation matched the total treatment zone. A point-by-point analysis of the corresponding locations on the refractive ablation map and the epithelial thickness map within the optical zone or the 6-mm diameter zone, when the optical zone was larger than 6 mm, was executed by the surgeon. Four locations within the central 2-mm area, four locations for each superior, inferior, temporal, and nasal 2- to 6-mm paracentral segment, and the location with the thickest epithelium were analyzed. At the location where the epithelial thickness exceeded the refractive ablation depth the

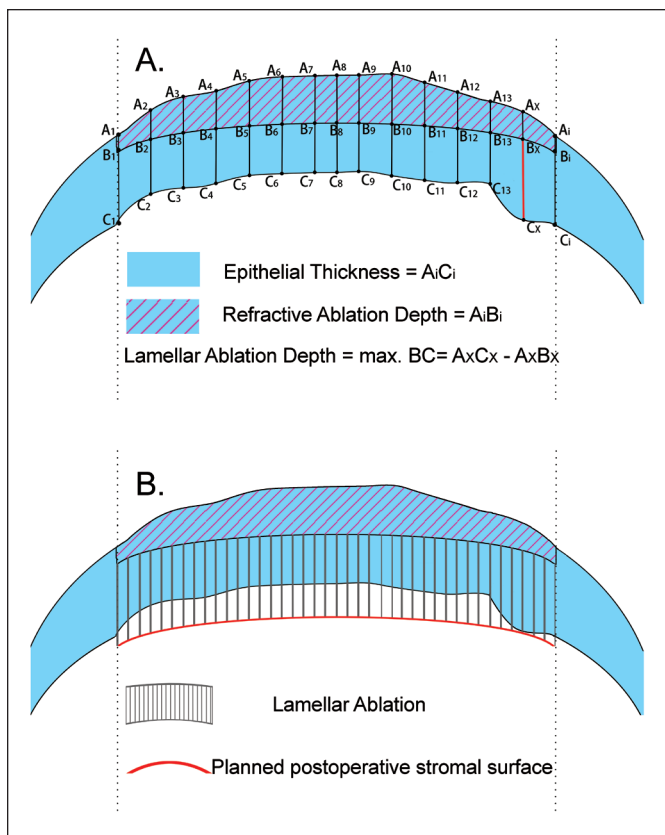


Figure 1. Schematic drawing illustrating the process of programming of the lamellar ablation depth. (A) Irregular epithelial thickness profile after primary refractive surgery derived by optical coherence tomography and refractive ablation plan profile, derived from corneal topography and patient's subjective refraction. The epithelial thickness (A_iC_i) and depth of ablation (A_iB_i) at corresponding locations are compared. At the location where the epithelial thickness exceeded the refractive ablation depth the most (shown in red line), the refractive ablation depth was subtracted from the measured epithelial thickness, giving the depth of the lamellar part of the compound ablation ($\max BC = A_xC_x - A_xB_x$). (B) Lamellar ablation and planned postoperative stromal surface.

most, the refractive ablation depth was subtracted from the measured epithelial thickness, giving the depth of the lamellar part of the compound ablation. This ensured that the treatment would “reach” the stroma at all points, with no unnecessary amount of tissue ablated. **Figures 1-2** illustrate the schematic process of determination of the lamellar ablation depth and one clinical example of the ablation profile programming, respectively.

The ablation plan was executed using a 1-KHz, 0.6-mm, 250-mJ/cm² dual flying-spot laser (iRES). To prevent haze, 0.02% mitomycin C was applied to the cornea for 30 seconds after the treatment in cases with history of haze after the primary treatment. Finally, a bandage contact lens (Acuvue Oasys; Johnson & Johnson, New Brunswick, NJ) was applied and worn for

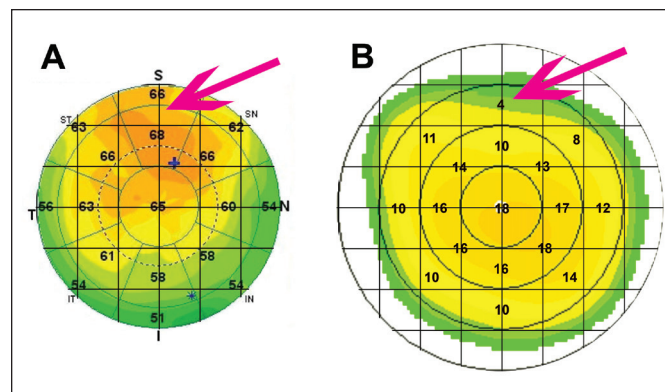


Figure 2. Ablation programming example in a case after laser in situ keratomileusis with subjective refraction of $-0.75 -0.50 \times 155$. (A) Significant epithelial thickening in the central and superior paracentral cornea. (B) Topography-guided ablation simulation with spherocylindrical correction according to subjective refraction. The average simulated ablation depth of the superior sector from a 2- to 3-mm radius was 4 μ m, whereas the epithelial thickness in the corresponding area was 66 to 68 μ m (shown with arrows). A 64- μ m lamellar ablation depth was programmed to ensure that the ablation would reach the stroma even under the thickest epithelium.

5 days or until complete reepithelialization was confirmed. The detailed surgical protocol has been described elsewhere.^{16,17}

DATA ANALYSIS

All visual acuity values were recorded as Snellen values and converted to logMAR units for statistical analysis and then converted back to Snellen values for presentation purposes.

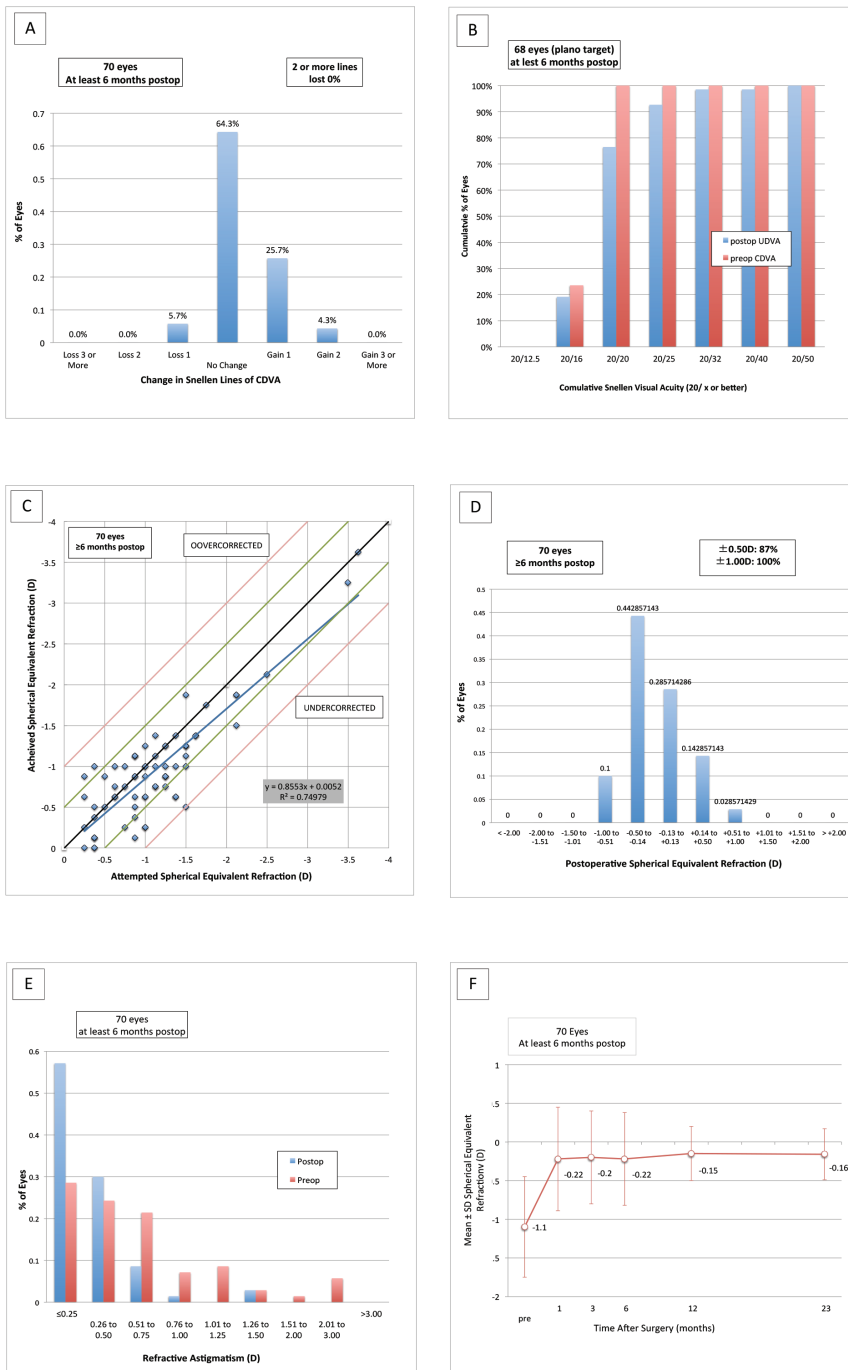
Vector analysis was used to analyze the changes in astigmatism according to the Alpíns method.¹⁸ Target induced astigmatism (vector of intended change in cylinder) and surgically induced astigmatism (vector of the actual change in cylinder) were evaluated. Cylinder values were kept in minus format.

Statistical analysis was performed using SPSS software (version 13.0; IBM Corporation, Armonk, NY). The paired *t* test and related-samples Wilcoxon signed-ranks test were used to compare the preoperative and postoperative parameters with normal distribution and non-normal distribution, respectively. A *P* value of less than .05 was considered statistically significant.

RESULTS

All 70 eyes were available for postoperative evaluation at 13.6 ± 9.4 months (range: 6 to 51 months) after the re-treatment, of which 57% ($n = 40$) were evaluated at 12 months or later. The maximal diameter of the optical zone was 5.88 ± 0.83 mm and the maximal diameter of the treatment zone was 8.14 ± 0.54 mm. The maximal ablation depth of the refractive compo-

Figure 3. (A) Change in Snellen line corrected distance visual acuity (CDVA) at last follow-up visit. (B) Cumulative postoperative uncorrected distance visual acuity (UDVA) and preoperative CDVA. (C) Attempted vs achieved spherical equivalent (SE). (D) SE refractive accuracy. (E) Preoperative and postoperative refractive astigmatism. (F) Stability of SE refraction. D = diopters



ment was $34.74 \pm 12.74 \mu\text{m}$. The ablation depth of the lamellar component was $61.78 \pm 7.95 \mu\text{m}$.

SAFETY

Figure 3A shows the change in the Snellen lines of CDVA. At their most recent follow-up visit, no eye lost two or more lines. CDVA improved from 20/17 to 20/16 ($P = .003$), yielding a safety index of 1.05.

There were no significant sight-threatening complications. No case of ocular infection was reported postoperatively. Two eyes (2.9%) presented with a trace of haze at 1 month postoperatively, in which spontaneous clearance was registered at the 3-month follow-up for both cases. Eyes with late-onset corneal haze were not observed in this cohort. In addition, two cases (2.9%) reported mild diplopia and four cases (5.7%)

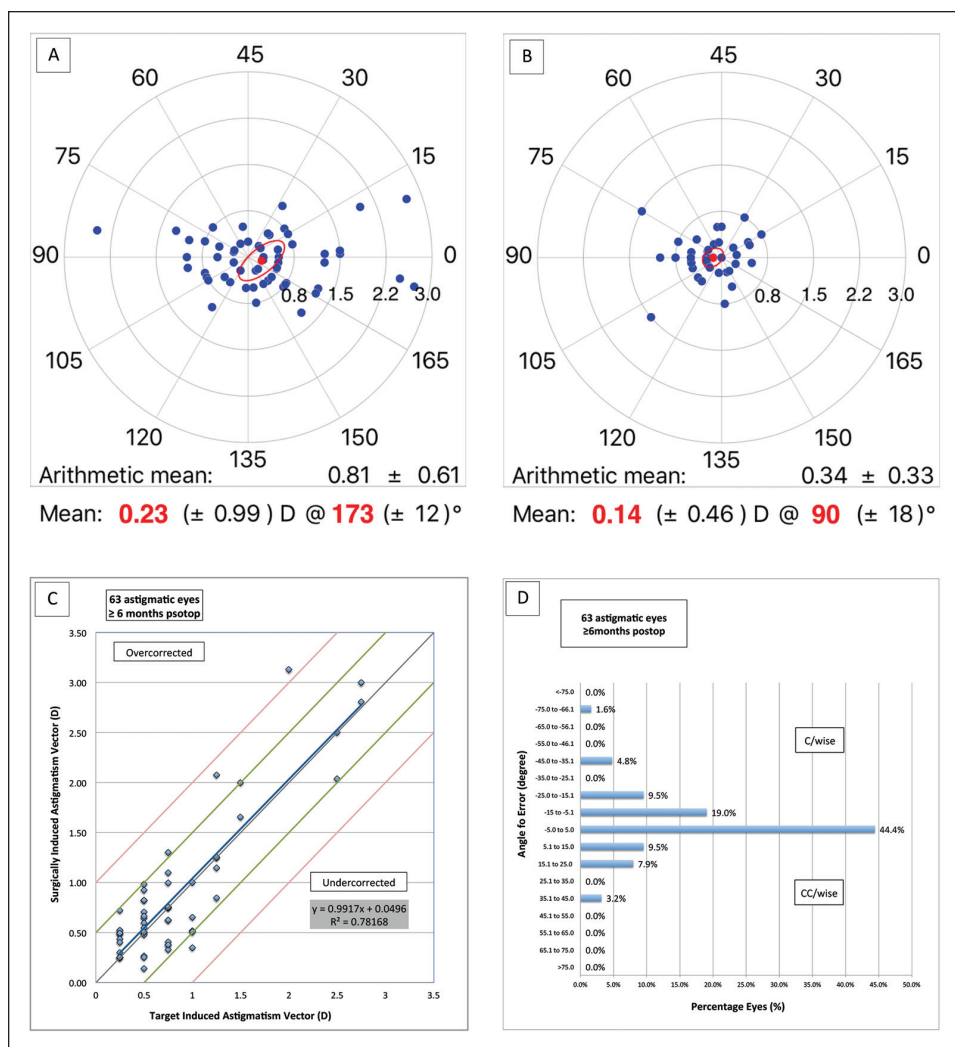


Figure 4. (A) Double-angle plot showing magnitude and angle of manifest astigmatism before enhancement. (B) Double-angle plot showing magnitude and angle of manifest astigmatism after enhancement. (C) Target induced astigmatism vs surgically induced astigmatism. (D) Angle of error of manifest astigmatism. D = diopters

had mild to moderate dry eye after the re-treatment at their most recent follow-up visit.

EFFICACY

Two eyes that were not targeted for emmetropia were excluded from the efficacy analysis. The cumulative data on postoperative UDVA compared to preoperative CDVA are shown in **Figure 3B**. At the most recent follow-up visit, the UDVA was 20/20 or better in 76.5% of cases (n = 52) and 20/40 or better in 98.5% of cases (n = 67). The efficacy index was 0.92.

PREDICTABILITY

The mean spherical equivalent was reduced from -1.10 ± 0.65 diopters (D) (range: -3.63 to -0.25 D) to -0.16 ± 0.34 D (range: -1.00 to +0.63 D). Of all eyes, 87% (n = 61) were within ± 0.50 D of the intended refraction and 100% (n = 70) were within ± 1.00 D (**Figures 3C-3D**).

PREDICTABILITY OF MANIFEST ASTIGMATISM CORRECTION

Seven eyes with zero preoperative astigmatism and no astigmatism correction were excluded from the astigmatism analysis. The preoperative and postoperative manifest astigmatism in 63 cases are demonstrated in **Figure 3E** and in double-angle plots (**Figures 4A-4B**). The mean magnitude of error and angle of error at the last follow-up visit were -0.04 ± 0.32 D (range: -0.65 to +1.13 D) and -1.40 ± 15.49 degrees (range: -43.15 to 45.00 degrees), respectively (**Figures 4C-4D**).

STABILITY

The stability of refraction is shown in **Figure 3F**. Postoperative spherical equivalent refraction stability was achieved at 1 month, with no statistically significant difference between each two follow-up points thereafter ($P = .912, .911, .971$, and $.844$, between 1 and 3 months, 3 and 6 months, 6 months and 1 year, and 1 year and the last follow-up, respectively).

TABLE 1
Preoperative and Postoperative HOAs and Asphericity (Mean \pm Standard Deviation)

Time	Total HOAs	HOAs (3rd + 5th)	HOAs (4th + 6th)	Asphericity
Preoperative	0.62 \pm 0.41	0.49 \pm 0.33	0.36 \pm 0.30	0.69 \pm 0.73
Postoperative	0.50 \pm 0.24	0.40 \pm 0.18	0.27 \pm 0.20	0.66 \pm 0.74
<i>P</i>	.021	.040	.030	.662

HOAs = higher order aberrations

HOAs AND ASPHERICITY

We analyzed ocular HOAs up to the sixth order within a 6-mm diameter and anterior corneal asphericity within a 3-mm diameter. The re-treatment reduced both total root mean square, odd-order (third + fifth), and even-order (fourth + sixth) HOAs significantly. Central anterior corneal asphericity remained unchanged (Table 1).

CORNEAL EPITHELIAL THICKNESS PROFILE

The epithelial thickness profile was analyzed in both the central 2-mm area and 2- to 5-mm paracentral area. Before re-treatment, the epithelium was 2.03 μ m thicker in the central area (60.96 \pm 5.48 mm) compared to that of the paracentral area (58.93 \pm 6.64 mm) ($P < .001$). After re-treatment, the epithelium in the paracentral area (62.19 \pm 5.37 mm) was 0.85 μ m thicker compared to that of the central area (61.34 \pm 6.22 mm) ($P = .002$).

DISCUSSION

Several mechanisms have been proposed as the cause of residual refractive errors after excimer laser refractive surgery, among which corneal biological diversity, including stromal healing response and epithelial remodeling, are thought to be major factors.¹⁹ Different options are available for enhancement, among which flap-relift LASIK has been most widely used for re-treatment after primary LASIK,^{1,20-22} due to the good outcomes, quick visual recovery, and ease of the procedure. The major complication of this procedure is epithelial ingrowth,^{1,21,22} whereas the major drawback is further decrease of residual stromal bed thickness. Surface ablation is another good alternative and is preferred in cases where reduction of the residual stromal thickness would compromise preservation of the corneal biomechanical strength and where flap-relift is estimated to be difficult or risky (eg, increased risk of epithelial ingrowth).

The refractive outcomes of re-treatment procedures are usually inferior to those of primary refractive surgery. The induction of HOAs⁸ and change in corneal physiological asphericity⁹ by the primary procedure decrease the efficacy and predictability of re-treatment. Therefore, customized re-treatment with topography-

or wavefront-guided ablation may be more effective in an enhancement procedure.

One of the main issues in planning topography-guided treatments is the possible discrepancy between the subjective and topographic cylinders.^{23,24} Studies demonstrated that analysis of the origin of the subjective astigmatism by accounting for the respective influence of the lenticular astigmatism, corneal odd-order aberrations,²⁵ and posterior corneal astigmatism²⁶ is crucial in determining the astigmatic end-point in topography-guided treatments.

Epithelial thickness profile change after primary laser refractive surgery was another important factor to be considered in re-treatment, especially with the topography-guided approach. Due to the flattened stroma after primary myopic ablation, the postoperative epithelium thickness over the central area increases as a compensatory response after LASIK,¹⁰ PRK,¹¹ and SMILE.¹² In the current study, the average epithelial thickness before re-treatment was thicker in both the central and paracentral areas compared to virgin cornea²⁷ and the central epithelium was significantly thicker than that of the paracentral area by 2.03 μ m. The unevenly thickened epithelium affected the corneal topography significantly, introducing inconformity between the anterior corneal surface covered by the epithelium and the stromal surface, in terms of astigmatism, irregularities, and asphericity.¹³ Under such circumstances, if conventional topography-guided PRK preceded by complete epithelial removal had been selected for the re-treatment, a topography-guided ablation profile, based on the corneal topography with epithelium-on, would have been incorrectly applied on the stromal surface containing different irregularities and curvature, consequently introducing ablation error and suboptimal outcomes.²⁸

The transepithelial topography-guided surface ablation used in the current study consists of: (1) the custom refractive component for treatment of the residual myopia, astigmatism, and corneal HOAs and (2) the PTK/lamellar component, containing both the epithelium and the protruding, remodeled stromal irregularities. That way the positive effect of the epithelial remodeling is preserved and the issue of nonconformity

between the stromal surface and the measured corneal surface^{16,29} is circumvented. Under such circumstances, if the epithelial thickness was underestimated, it would leave a part of the stroma only partially treated, whereas an overestimation of the epithelial thickness would lead to unnecessary waste of corneal tissue. Epithelial mapping–assisted transepithelial topography-guided ablation addressed this issue.

The proportions of ablated epithelium and stroma in the lamellar component are different at different points on the cornea, especially in corneas with an irregular stromal surface and highly irregular epithelial thickness profile. In eyes with previous myopic treatment, the epithelium will usually be thicker centrally to partially compensate for the stromal tissue removal, and thinner paracentrally to partially compensate for the biomechanical stromal thickening.^{10,30,31} A transepithelial PTK ablation will thus break through the thinner peripheral epithelium, resulting in stromal ablation in the periphery while still ablating epithelium in the center. Under the assumption that a similar epithelial remodeling as after the primary treatment would occur after the re-treatment, this would have a hyperopic treatment effect (a myopic shift) and would affect the nomogram for a transepithelial PRK re-treatment. However, the epithelium will regenerate after surgery with a thickness profile defined by the curvature gradient of the new stromal surface.^{10,30–32} Therefore, the difference between the epithelial thickness profile before and after the transepithelial PRK treatment will also contribute a refractive shift.

The topography-guided ablation profile in the current study uses a wide transition zone with a gradual dioptric change from treated to untreated cornea that is designed to create a consistent curvature gradient on the stromal surface, meaning that the epithelial thickness profile is more likely to return to the appearance of a virgin untreated cornea within the central optically active zone, because only the unevenness of the stromal curvature gradient leads to an uneven epithelial thickness profile. If the uneven gradient change is removed, the epithelium should be expected to return without a “lenticule” configuration (**Figure A**, available in the online version of this article). If this is achieved, the refractive shift induced by the peripheral stromal ablation from the transepithelial PTK is balanced by the refractive shift due to the change in the epithelial thickness profile, resulting in a refractive-neutral effect, and there does not need to be a change to the nomogram. Such a conclusion has also been supported by the results of the current study. This goal may only be achieved for myopic corrections up to a certain limit because of the tissue constraints of

the human cornea when the final myopic correction is higher than a certain amount where it seems impossible to have a completely regular gradient change (eg, -10.00 D).

The difference in the ablation rate between the epithelium and the stroma may induce an ablation error in transepithelial ablation and influence the predictability of postoperative refraction. But even if the achieved ablation is equal to the planned ablation, a factor not accounted for would be the effect of the different epithelial and stromal refractive indexes after redistribution of the relative amounts and shapes of the epithelium and stroma that occurs with the current transepithelial treatment. This redistribution may cause the change in both local and global corneal refractive indexes and may account for a certain additional postoperative refractive change. This is in line with the findings of Reinstein et al.,^{15,33} who reported myopic or hyperopic shift after PTK in the treatment of corneas with irregular irregularities.

Epithelial thickness mapping–assisted PTK followed by wavefront- or topography-guided custom ablation has been used in treatment of highly irregular corneas.^{14,15} As an alternative to the current concept, ablation based on stromal surface topography after epithelial removal is another proper solution for cases with epithelial remodeling. Treatment of highly aberrated corneas using intraoperative stromal topography-based, wavefront-guided ablation, after removal of the epithelium,³⁴ and stromal surface topography-guided custom ablation in a post-LASIK flap complication case, where the stromal surface information was obtained by subtracting the very high-frequency digital ultrasound-derived epithelial thickness profile from the Orbscan-derived corneal front surface elevation,³⁵ have been reported with satisfactory refractive outcomes.

In our transepithelial treatments, special attention was given to the following three conditions to minimize the discrepancy between the planned and achieved ablation: (1) use of excimer laser with radial ablation efficiency compensation; (2) ablation planning that takes into account the different ablation rates between the epithelium and the stroma; and (3) design of a smooth transition to contribute to a refractive-neutral postoperative epithelial thickness profile. We presume that the increase in the epithelial thickness smoothness was achieved due to the wide and smooth customized transition between the treated and untreated cornea, as well as the smoothing of the underlying stromal surface created by topography-guided ablation used in the ablation design.^{31,32}

The issue of postoperative haze used to be an argument against surface ablation for enhancements after laser refractive surgery.³⁶ Since the use of mitomycin

C became prevalent, the incidence of severe haze has declined steadily, whereas the increased smoothness of the ablated surface with modern, small flying spot lasers also seems to play an important role.³⁷ In the current study, due to the smooth stromal surface created by the 0.5-mm spot laser, the low postoperative ambient ultraviolet exposure in subarctic Norway, preoperative and postoperative use of vitamin C, and intraoperative use of mitomycin C in cases with history of haze after the primary treatment, only a trace of haze at 1 month postoperatively was registered in two cases.

The incidence of infection after surface ablation has been reported to be higher than after LASIK, and Gram-positive organisms are the most common pathogens.^{38,39} Patients enrolled in the study all received antibiotic prophylaxis with broad spectrum, including Gram-positive coverage (ciprofloxacin 0.5%, Cilox; Alcon Laboratories, Inc., Fort Worth, TX), and a detailed education on postoperative ocular hygiene, as well as confirmation of total reepithelialization on slit-lamp before bandage contact lens removal. No postoperative infection was reported in our case series.

Compared with studies on re-treatment of residual refractive error after previous refractive surgery (Table A, available in the online version of this article) published in the past 10 years,^{1,6,20-22,40-46} our procedure showed favorable outcomes in terms of safety, efficacy, and predictability.

To the best of our knowledge, this is the first study using transepithelial topography-guided, epithelial mapping-assisted ablation featuring a customized wide and smooth transition zone that contributes to even postoperative epithelial remodeling with negligible refractive contribution. It appears to be safe and highly effective for addressing myopic regression in patients who have previously undergone myopic refractive surgery.

AUTHOR CONTRIBUTIONS

Study concept and design (WZ, SC, AS); data collection (WZ, YX); analysis and interpretation of data (WZ, DZR, TPU); writing the manuscript (WZ, AS); critical revision of the manuscript (DZR, XC, SC, YX, TPU); statistical expertise (TPU); administrative, technical, or material support (SC); supervision (AS)

REFERENCES

1. Saeed A, O'Doherty M, O'Doherty J, O'Keefe M. Analysis of the visual and refractive outcome following laser in situ keratomileusis (LASIK) retreatment over a four-year follow-up period. *Int Ophthalmol*. 2007;27:23-29.
2. Brahma A, McGhee CN, Craig JP, et al. Safety and predictability of laser in situ keratomileusis enhancement by flap reelevation in high myopia. *J Cataract Refract Surg*. 2001;27:593-603.
3. Pokroy R, Mimouni M, Sela T, Munzer G, Kaiserman I. Myopic laser in situ keratomileusis retreatment: Incidence and associations. *J Cataract Refract Surg*. 2016;42:1408-1414.
4. Mohammadi SF, Nabovati P, Mirzajani A, Ashrafi E, Vakilian B. Risk factors of regression and undercorrection in photorefractive keratectomy: a case-control study. *Int J Ophthalmol*. 2015;8:933-937.
5. Pokroy R, Mimouni M, Sela T, Munzer G, Kaiserman I. Predictors of myopic photorefractive keratectomy retreatment. *J Cataract Refract Surg*. 2017;43:825-832.
6. Reinstein DZ, Carp GI, Archer TJ, Vida RS. Outcomes of retreatment by LASIK after SMILE. *J Refract Surg*. 2018;34:578-588.
7. Siedlecki J, Luft N, Mayer WJ, et al. CIRCLE enhancement after myopic SMILE. *J Refract Surg*. 2018;34:304-309.
8. Padmanabhan P, Mrochen M, Basuthkar S, Viswanathan D, Joseph R. Wavefront-guided versus wavefront-optimized laser in situ keratomileusis: contralateral comparative study. *J Cataract Refract Surg*. 2008;34:389-397.
9. Hersh PS, Fry K, Blaker JW. Spherical aberration after laser in situ keratomileusis and photorefractive keratectomy: clinical results and theoretical models of etiology. *J Cataract Refract Surg*. 2003;29:2096-2104.
10. Reinstein DZ, Archer TJ, Gobbe M. Change in epithelial thickness profile 24 hours and longitudinally for 1 year after myopic LASIK: three-dimensional display with Artemis very high-frequency digital ultrasound. *J Refract Surg*. 2012;28:195-201.
11. Hou J, Wang Y, Lei Y, Zheng X, Zhang Y. Corneal epithelial remodeling and its effect on corneal asphericity after transepithelial photorefractive keratectomy for myopia. *J Ophthalmol*. 2016;2016:8582362.
12. Luft N, Ring MH, Dirisamer M, et al. Corneal epithelial remodeling induced by small incision lenticule extraction (SMILE). *Invest Ophthalmol Vis Sci*. 2016;57:176-183.
13. Salah-Mabed I, Saad A, Gatineau D. Topography of the corneal epithelium and Bowman layer in low to moderately myopic eyes. *J Cataract Refract Surg*. 2016;42:1190-1197.
14. Reinstein DZ, Archer T. Combined Artemis very high-frequency digital ultrasound-assisted transepithelial phototherapeutic keratectomy and wavefront-guided treatment following multiple corneal refractive procedures. *J Cataract Refract Surg*. 2006;32:1870-1876.
15. Reinstein DZ, Archer TJ, Dickeson ZI, Gobbe M. Transepithelial phototherapeutic keratectomy protocol for treating irregular astigmatism based on population epithelial thickness measurements by artemis very high-frequency digital ultrasound. *J Refract Surg*. 2014;30:380-387.
16. Chen X, Stojanovic A, Zhou W, Utheim TP, Stojanovic F, Wang Q. Transepithelial, topography-guided ablation in the treatment of visual disturbances in LASIK flap or interface complications. *J Refract Surg*. 2012;28:120-126.
17. Stojanovic A, Chen S, Chen X, et al. One-step transepithelial topography-guided ablation in the treatment of myopic astigmatism. *PLoS One*. 2013;8:e66618.
18. Alpíns N. Astigmatism analysis by the Alpíns method. *J Cataract Refract Surg*. 2001;27:31-49.
19. Moshirfar M, Desautels JD, Walker BD, et al. Mechanisms of optical regression following corneal laser refractive surgery: epithelial and stromal responses. *Med Hypothesis Discov Innov Ophthalmol*. 2018;7:1-9.
20. Bragheeth MA, Fares U, Dua HS. Re-treatment after laser in situ

keratomileusis for correction of myopia and myopic astigmatism. *Br J Ophthalmol*. 2008;92:1506-1510.

21. McAlinden C, Moore JE. Retreatment of residual refractive errors with flap lift laser in situ keratomileusis. *Eur J Ophthalmol*. 2011;21:5-11.
22. Schallhorn SC, Venter JA, Hannan SJ, Hettinger KA, Teenan D. Flap lift and photorefractive keratectomy enhancements after primary laser in situ keratomileusis using a wavefront-guided ablation profile: refractive and visual outcomes. *J Cataract Refract Surg*. 2015;41:2501-2512.
23. Kanellopoulos AJ. Topography-modified refraction (TMR): adjustment of treated cylinder amount and axis to the topography versus standard clinical refraction in myopic topography-guided LASIK. *Clin Ophthalmol*. 2016;10:2213-2221.
24. Alpíns N. Topography-modified refraction: adjustment of treated cylinder amount and axis to the topography versus standard clinical refraction in myopic topography-guided LASIK. *Clin Ophthalmol*. 2017;11:1203-1204.
25. Zhou W, Stojanovic A, Utheim TP. Assessment of refractive astigmatism and simulated therapeutic refractive surgery strategies in coma-like-aberrations-dominant corneal optics. *Eye Vis (Lond)*. 2016;3:13.
26. Koch DD, Ali SF, Weikert MP, Shirayama M, Jenkins R, Wang L. Contribution of posterior corneal astigmatism to total corneal astigmatism. *J Cataract Refract Surg*. 2012;38:2080-2087.
27. Reinstein DZ, Archer TJ, Gobbe M, Silverman RH, Coleman DJ. Epithelial thickness in the normal cornea: three-dimensional display with Artemis very high-frequency digital ultrasound. *J Refract Surg*. 2008;24:571-581.
28. Reinstein DZ, Archer TJ, Gobbe M. Improved effectiveness of transepithelial PTK versus topography-guided ablation for stromal irregularities masked by epithelial compensation. *J Refract Surg*. 2013;29:526-533.
29. Stojanovic A, Zhang J, Chen X, Nitter TA, Chen S, Wang Q. Topography-guided transepithelial surface ablation followed by corneal collagen cross-linking performed in a single combined procedure for the treatment of keratoconus and pellucid marginal degeneration. *J Refract Surg*. 2010;26:145-152.
30. Reinstein DZ, Silverman RH, Raevsky T, et al. Arc-scanning very high-frequency digital ultrasound for 3D pachymetric mapping of the corneal epithelium and stroma in laser in situ keratomileusis. *J Refract Surg*. 2000;16:414-430.
31. Reinstein DZ, Archer TJ, Gobbe M. Rate of change of curvature of the corneal stromal surface drives epithelial compensatory changes and remodeling. *J Refract Surg*. 2014;30:799-802.
32. Vinciguerra P, Roberts CJ, Albé E, et al. Corneal curvature gradient map: a new corneal topography map to predict the corneal healing process. *J Refract Surg*. 2014;30:202-207.
33. Reinstein DZ, Archer TJ, Gobbe M. Refractive and topographic errors in topography-guided ablation produced by epithelial compensation predicted by 3D Artemis VHF digital ultrasound stromal and epithelial thickness mapping. *J Refract Surg*. 2012;28:657-663.
34. Vinciguerra P, Camesasca FI. Custom phototherapeutic keratectomy with intraoperative topography. *J Refract Surg*. 2004;20:S555-S563.
35. Reinstein DZ, Gobbe M, Archer TJ, Youssefi G, Sutton HF. Stromal surface topography-guided custom ablation as a repair tool for corneal irregular astigmatism. *J Refract Surg*. 2015;31:54-59.
36. Carones F, Vigo L, Carones AV, Brancato R. Evaluation of photorefractive keratectomy retreatments after regressed myopic laser in situ keratomileusis. *Ophthalmology*. 2001;108:1732-1737.
37. Vinciguerra P, Camesasca FI, Torres IM. Transition zone design and smoothing in custom laser-assisted subepithelial keratectomy. *J Cataract Refract Surg*. 2005;31:39-47.
38. Donnenfeld ED, O'Brien TP, Solomon R, Perry HD, Speaker MG, Wittmann J. Infectious keratitis after photorefractive keratectomy. *Ophthalmology*. 2003;110:743-747.
39. Schallhorn JM, Schallhorn SC, Hettinger K, Hannan S. Infectious keratitis after laser vision correction: incidence and risk factors. *J Cataract Refract Surg*. 2017;43:473-479.
40. Cagil N, Aydin B, Ozturk S, Hasiripi H. Effectiveness of laser-assisted subepithelial keratectomy to treat residual refractive errors after laser in situ keratomileusis. *J Cataract Refract Surg*. 2007;33:642-647.
41. Beerthuis JJ, Siebelt E. Surface ablation after laser in situ keratomileusis: retreatment on the flap. *J Cataract Refract Surg*. 2007;33:1376-1380.
42. Saeed A, O'Doherty M, O'Doherty J, O'Keefe M. Laser-assisted subepithelial keratectomy retreatment after laser in situ keratomileusis. *J Cataract Refract Surg*. 2008;34:1736-1741.
43. Garcia-Gonzalez M, Teus MA. Creation of a new femtosecond laser-assisted mini-flap to enhance late regression after LASIK. *J Refract Surg*. 2013;29:564-568.
44. Ng-Darjuan MF, Evangelista RP, Agahan AL. Photorefractive keratectomy with adjunctive mitomycin C for residual error after laser-assisted in situ keratomileusis using the Pulzar 213 nm solid-state laser: early results. *ISRN Ophthalmol*. 2013;2013:815840.
45. Lee BS, Gupta PK, Davis EA, Hardten DR. Outcomes of photorefractive keratectomy enhancement after LASIK. *J Refract Surg*. 2014;30:549-556.
46. Broderick KM, Sia RK, Ryan DS, et al. Wavefront-optimized surface retreatments of refractive error following previous laser refractive surgery: a retrospective study. *Eye Vis (Lond)*. 2016;3:3.

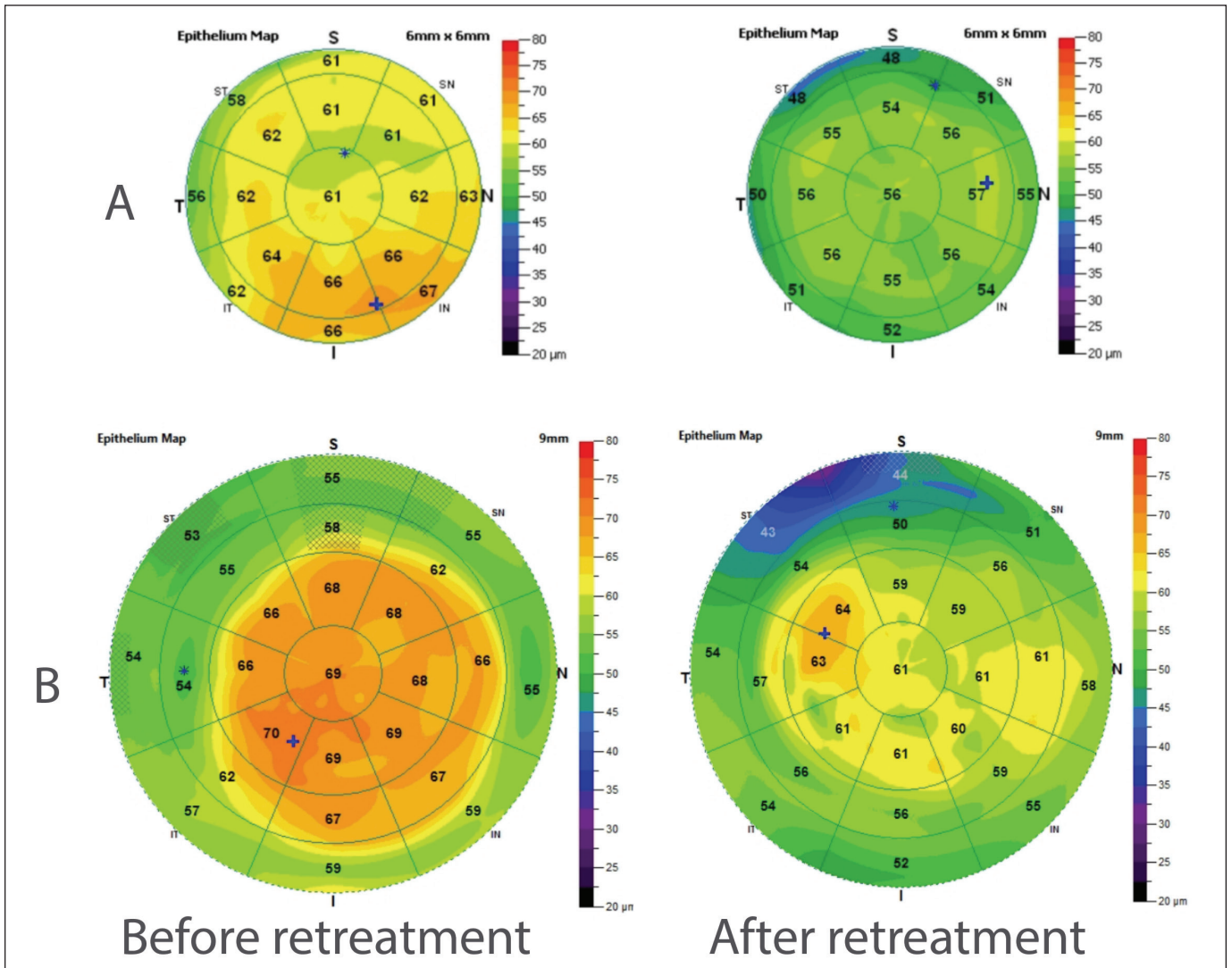


Figure A. Epithelial thickness map (ETM) in two cases before and after the transepithelial photorefractive keratectomy (PRK), showing the change from a positive epithelium lenticule before surgery to an epithelium with no power after surgery. Case A: 6-mm ETM taken by RT-Vue 100, OptoVue OCT (OptoVue, Fremont, CA) and case B: 9-mm ETM taken by Avanti, OptoVue OCT.

TABLE A

Studies on Enhancement of Residual Refractive Errors After Previous Refractive Surgery

Study	No. of Eyes	Type of Primary Surgery	Re-treatment Technology	Mean Follow-up Time (mo)	SI	EI	Predictability [% of Eyes]		Complications	
							Within ± 0.50 D	Within ± 1.00 D	Haze	Others
Cagil et al., 2007	24	LASIK	LASEK	11.5	1.04	0.87	65.5	83.3	Significant haze developed in 20.8% of eyes	None
Beerthuizen & Siebelt, 2007	18	LASIK	WF-guided LASEK or PRK	12	1	0.87	83	100	Severe late-onset haze in 11.1% of eyes	None
Saeed et al. 2007	60	LASIK	LASIK with flap-relift	22.3	1	0.85	77	83	-	Epithelial ingrowth in 5% of eyes; night vision problems in 11% of eyes; dry eye in 6% of eyes
Saeed et al., 2008	22	LASIK	LASEK	6.7	1	0.83	55.4	77.3	Haze with grade ≤ 1 in 45.4% of eyes	-
Bragheeth et al., 2008	32	LASIK	LASIK with flap-relift	12	-	-	56	78	-	Epithelial ingrowth in 6% of eyes
McAlinden & Moore, 2011	60	LASIK	WF-guided LASIK with flap-relift	6	0.98	0.92	88.3	98.3	-	Epithelial ingrowth in 23% of eyes; dry eye in 8% of eyes
Garcia-Gonzalez & Teus, 2013	10	LASIK	LASIK with new FS-assisted mini flap	6	0.99	0.90	100	100	0	0
Ng-Darjuan et al., 2013	16	LASIK	Topography-guided PRK with solid-state laser	6	-	-	56	94	0	-
Lee et al., 2014	29	LASIK	PRK	19.5	0.95	0.82	-	-	Clinically significant haze in 2.3% of eyes	DLK in 11.6% of eyes
Lee et al., 2014	119	LASIK	WF-guided LASIK with flap-relift	4	1.03	0.93	87.4	99.2	0	Epithelial ingrowth in 1.7% of eyes
Schallhorn et al., 2015	171	FS-LASIK	WF-guided PRK	4.2	1	0.91	84.2	97.6	0	Dry eye and superficial punctate epithelial erosions in 1.8% of eyes
Broderick et al., 2016	120	78 PRK, 9 LASEK, 33 LASIK	WF-optimized PRK	6	1.03	0.84	78	96	0	0
Reinstein et al., 2018	116	SMILE	Thin-flap LASIK with side cut only or Circle technique	12	-	-	74	95	Trace of haze in 5% of eyes	No visually significant complications
Current study	70	38 PRK, 19 LASIK, 3 SMILE	Transepithelial topography-guided and epithelial mapping-guided custom ablation	13.6	1.05	0.92	87	100	Trace of haze in 2.9% of eyes	Mild diplopia in 2.9% of eyes; mild to moderate dry eye in 5.7% of eyes

SI = safety index; EI = efficacy index; SE = spherical equivalent; D = diopters; LASIK = laser in situ keratomileusis; LASEK = laser epithelial keratomileusis; WF = wavefront; PRK = photorefractive keratectomy; DLK = diffuse lamellar keratitis; FS-LASIK = femtosecond laser-assisted LASIK; SMILE = small incision lenticule extraction